Analysis of a probing control strategy

Velut, Stéphane; Hagander, Per

Published in:
Proceedings / American Control Conference 2003

DOI:
10.1109/ACC.2003.1239086

2003

LUND UNIVERSITY

PO Box 117
221 00 Lund
+46 46-222 00 00

Analysis of a probing control strategy

Stéphane Velut **Per Hagander**
Department of Automatic Control
Lund Institute of Technology
Box 118, SE-221 00 Lund, Sweden
{svelut,per}@control.lth.se

Abstract

In this paper we analyse an extremum controller based on a pulse technique. The idea is to superimpose probing pulses to the control signal and use for feedback the size of the pulse response in the output. The probing control strategy has been used with success for the control of the substrate feeding in *E. coli* cultivations, see [1]. The analysis is done here for systems of Hammerstein type with a piecewise affine nonlinearity. Stability of the closed-loop system can be checked by solving suitable linear matrix inequalities. Some performance analysis that can help the user for the control design is also performed.

1 Introduction

In extremum control, the task is to find and track the best operating point of a nonlinear process. The optimal setpoint is usually given by a nonlinear static input-output map presenting an extremum. There are also applications where it is desirable to drive the process to a saturation instead of an extremum. The classical approach consists in adding a known time-varying signal to the process input and correlating the output with the perturbation signal to get information about the nonlinearity gradient. The controller adjusts continuously the control signal towards the optimum.

In [8], the authors presented the stability analysis of an extremum seeking scheme for a general nonlinear dynamical system. Stability of the seeking scheme was proven under restrictive conditions: small adaptation gain and fast plant dynamic. In [7] they developped a tighter analysis where the process was modelled by a Wiener-Hammerstein system. No stability region was provided.

In [1] and [2] a probing controller based on a pulse technique is described. The main difference with the classical scheme is the separation in time of the correlation/probing phase and the control phase. Pulses are periodically introduced at the process input and a control action is taken at the end of every pulse. This also allows the regulation of the output signal by manipulation of a second control variable between two successive pulses. The control algorithm has been implemented and tested on real plants where good performance could be achieved, see [1].

The objective of this paper is to provide a rigorous analysis for stability of the probing controller. The paper is organized as follows. In Section 2, we present an example that was at the origin of the probing controller. The problem is then formulated in a piecewise affine framework in Section 3. Stability and performance analysis is carried out in Section 4, using linear matrix inequalities. We finally apply the stability and the performance results on the example of Section 2.

2 Motivating example

Escherichia coli is a common host organism to produce recombinant proteins. It can be quickly grown to high cell densities and gives high production levels. A limiting factor is the formation of the byproduct acetate that has been reported to reduce cell growth and protein production. Formation of acetate occurs under anaerobic conditions but also under fully aerobic conditions when the carbon source–glucose– is in excess. Aerobic conditions can be guaranteed by manipulating the agitation speed in order to keep a constant dissolved oxygen concentration in the bioreactor. The main difficulty consists in finding the optimal feed rate. High feed rates result in

0-7803-7896-2/03/$17.00 ©2003 IEEE

Proceedings of the American Control Conference
Denver, Colorado June 4-6, 2003

short cultivation times but may result in overfeeding. The critical glucose concentration above which the respiratory capacity of the cells saturates and acetate is produced, is unknown and may vary during a cultivation. Furthermore, accurate online measurement of glucose concentration is not available. The idea of the probing approach is to detect the saturation of the respiration by superimposing pulses in the feed. The pulses give rise to changes in the glucose and oxygen uptake rates, that can be seen in the dissolved oxygen signal. The probing controller uses the size of the pulse response to adjust the feed rate. Figure 1 shows the complete scheme.

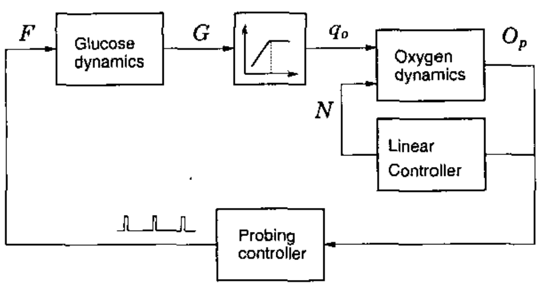

Figure 1: Block diagram of the closed-loop system. By making pulses in the feed rate F, it is possible to determine if the glucose concentration G is below or above the critical value G_{crit} when the oxygen uptake rate q_o starts to saturate. The agitation speed N regulates O_p between the pulses in F.

The closed-loop system is a multivariable setup with 2 inputs, the feed rate F, the agitation speed N and 1 output, the dissolved oxygen concentration O_p. The objective is to drive the system to the saturation and regulate the output close to a reference value.

The overall system is rather complex but the analysis is possible when the input dynamic is neglected. The periodic nature of the total controller, with one regulation phase followed by a probing phase, suggests a discrete-time description. We will also restrict the analysis to static nonlinearities that are piecewise linear. Global stability can thus be investigated by using tools for discrete-time piecewise linear systems.

3 Problem formulation

We assume that the process is a Hammerstein model: a static nonlinearity followed by a dynamical linear process, see Figure 2. A state space representation of the process can be written as

$$\begin{aligned} \dot{x} &= Ax + B_1 f(v) + B_2 w \quad x \in R^n \\ y &= Cx \end{aligned} \tag{1}$$

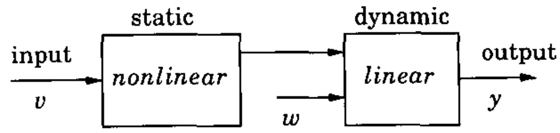

Figure 2: Hammerstein model

The probing controller gets information about the nonlinearity from pulses that are periodically superimposed to the control signal. The size of the pulse response, which depends on the local gain of the nonlinearity, is used to adjust the control signal.

The controller law can be written as:

$$\begin{aligned} u_{k+1} &= u_k + K[y((k+1)T) - y(kT+T_c) - y_r] \\ v(t) &= u_k + u_p(t) \qquad t \in [kT,\ kT+T] \end{aligned} \tag{2}$$

where v is the control signal and $u_p(t)$ is the T-periodic perturbation signal defined by:

$$\begin{aligned} u_p(t) &= 0 \qquad t \in [kT,\ kT+T_c) \\ u_p(t) &= u_p^0 \quad t \in [kT+T_c, (k+1)T) \end{aligned} \tag{3}$$

A reference value y_r is used for the desired pulse response. It is useful when the nonlinearity does not present an extremum but a saturation. Since the controller is time-periodic, one can regard the feedback system as a sampled data system where the sampling time is the period T of the perturbation signal.

During the control phase with length T_c, the process input v is kept constant while the second input w regulates the output y:

$$t \in [kT,\ kT+T_c) \begin{cases} \dot{x} = Ax + B_1 f(u_k) + B_2 w \\ \dot{x}_c = A_c x_c + B_c y \\ y = Cx \\ w = C_c x_c + D_c y \end{cases} \tag{4}$$

where $x_c \in R^m$ is the controller state of the second loop. After integration between kT and $kT + T_c$, we get

$$\begin{bmatrix} x(kT+T_c) \\ x_c(kT+T_c) \end{bmatrix} = A_{d1} \begin{bmatrix} x(kT) \\ x_c(kT) \end{bmatrix} + B_{d1} f(u_k) \tag{5}$$

where A_{d1} and B_{d1} are given in the appendix.

During the probing phase with length $T_p = T - T_c$, the control signal w is kept constant:

$$t \in [kT+T_c,\ kT+T) \begin{cases} \dot{x} = Ax + B_1 f(u_k + u_p^0) \\ \qquad + B_2 w(kT+T_c) \\ \dot{x}_c = 0 \\ y = Cx \end{cases} \tag{6}$$

After integration between $kT + T_c$ and $kT + T$, we get

$$\begin{bmatrix} x(kT+T) \\ x_c(kT+T) \end{bmatrix} = A_{d2} \begin{bmatrix} x(kT+T_c) \\ x_c(kT+T_c) \end{bmatrix} + B_{d2} f(u_k + u_p^0) \quad (7)$$

where A_{d2} and B_{d2} are given in the appendix.

Equations (2), (5) and (7) lead to the closed-loop system:

$$\begin{aligned} X_{k+1} &= A_d X_k + B_d \begin{bmatrix} f(u_k) \\ f(u_k + u_p^0) \end{bmatrix} + a_d \\ u_k &= [0 \ \ldots 0 \quad 1] X_k \end{aligned} \quad (8)$$

where

$$A_d = \begin{bmatrix} A_{d2}A_{d1} & 0 \\ KC_e(A_{d2}A_{d1} - A_{d1}) & 1 \end{bmatrix} \qquad X_k = \begin{bmatrix} x(kT) \\ x_c(kT) \\ u_k \end{bmatrix}$$

$$B_d = \begin{bmatrix} A_{d2}B_{d1} & B_{d2} \\ KC_e(A_{d2}B_{d1} - B_{d1}) & KC_eB_{d1} \end{bmatrix} \quad a_d = \begin{bmatrix} 0 \\ -Ky_r \end{bmatrix}$$

Assumption: the static nonlinearity f is a piecewise affine function defined on $p+1$ intervals.

The functions $f(\cdot)$ and $f(\cdot + u_p^0)$ in (8) then induce a partition of the state space into $2p+1$ polyhedral cells $\{\mathbf{X}_i\}_{i \in I}$. The regions $\mathbf{X}_i$ can be defined by the matrices E_i and e_i such that:

$$\mathbf{X}_i = \{X \in R^{n+m+1}, \ \ E_i X + e_i \succeq 0\}$$

where the inequality $\succeq$ should be taken componentwise.

The closed-loop system has a piecewise affine structure and can be represented by:

$$X_{k+1} = A_i X_k + a_i, \ \ \text{for} X_k \in \mathbf{X}_i, \ \ i \in I$$

We assume that the closed-loop system has a unique equilibrium, that is shifted such that it coincides with the origin.

4 Stability and performance analysis

Stability analysis of the closed-loop system can be done using piecewise quadratic Lyapunov functions as in [5] or [6] in continuous time and [3] or [4] in discrete time. Since the probing controller (2) contains one integrator, the convergence of the closed-loop system may not be globally exponential. Local analysis can still be carried out using LMIs, but we choose to change the integrator to a pole at $z = 0.99$ and perform global analysis.

4.1 Stability

The Lyapunov function candidate is piecewise quadratic:

$$V(X) = \bar{X}^T \bar{P}_i \bar{X} \quad \text{for } X \in \mathbf{X}_i, \ i \in I$$

where $\bar{P}_i$ is a symmetric matrix and $\bar{X}$ denotes the state vector augmented by 1:

$$\bar{X} = \begin{bmatrix} X \\ 1 \end{bmatrix}$$

Stability can be tested by checking that the following linear matrix inequalities are feasible

$$\begin{aligned} &\bar{P}_i - g_i \bar{G}_i > 0, && i \in I \\ &\bar{A}_i^T \bar{P}_j \bar{A}_i - \bar{P}_i + h_{ij}\bar{G}_i + k_{ij}\bar{G}_{ij} < 0, && i, \ j \in I \\ &g_i > 0, \ \ h_{ij} > 0, \ \ k_{ij} > 0, && i, \ j \in I \end{aligned}$$

where

$$\bar{A}_i = \begin{bmatrix} A_i & a_i \\ 0 & 1 \end{bmatrix}$$

The so-called S–procedure [9] has been used to reduce the conservativness of the LMIs:

- the matrix $\bar{G}_i$ is used to restrict the domain of validity for LMIs to the cell $\mathbf{X}_i$. It takes the form

$$\bar{G}_i = \begin{bmatrix} 0 & .5E_i^T \\ .5E_i & e_i \end{bmatrix}$$

- the relaxation term $\bar{G}_{ij}$ describes when a switch from the cell X_i to the cell X_j is possible in one step:

$$\bar{X}_k^T (h_i \bar{G}_i + k_{ij} \bar{G}_{ij}) \bar{X}_k > 0$$
$$\text{when } X_k \in \mathbf{X}_i \text{ and } X_{k+1} \in \mathbf{X}_j$$

We use a matrix $\bar{G}_{ij}$ of the following form:

$$\bar{G}_{ij} = \begin{bmatrix} 0 & .5A_i^T E_j^T \\ .5E_j A_i & e_j + E_j A_i \end{bmatrix}$$

4.2 Performance

We will now present a way to estimate the closed-loop performance. A natural performance objective could be to minimize the quadratic cost $J(X_0)$ defined by

$$J(X_0) = \sum_{k=0}^{\infty} X_k^T Q_i X_k, \quad i \in I$$

An upper bound on $J(X_0)$ can be derived by solving suitable linear matrix inequalities. We have indeed the following result:

Theorem 1 *Assume existence of symmetric matrices $\bar{P}_i$ and positive scalars g_i, $k_{ij} > 0$ such that*

$$\bar{P}_i - g_i\bar{G}_i > 0, \qquad i \in I$$
$$\bar{A}_i^T\bar{P}_j\bar{A}_i - \bar{P}_i + k_{ij}\bar{G}_{ij} + \bar{Q}_i < 0 , \qquad i,\ j \in I$$

then

$$J(X_0) < \bar{X_0}^T\bar{P}_{i_0}\bar{X}_0, \quad X_0 \in \mathbf{X}_{i_0}$$

The proof is similar to that in the continuous case, see [5].

A better upper bound can be obtained by finding P_{i_0} that minimizes $V(X_0)$.

$$P_{i_0}^* = \arg \inf_{P_{i_0}} \bar{X_0}^T\bar{P}_{i_0}\bar{X}_0$$

Note that although the optimization is done for a specific intial state X_0, the matrix $\bar{P}_{i0}$ gives a bound on the cost for all initial states in the partition. A lower bound can be derived similarly by replacing $\bar{Q}_i$ in the analysis by $-\bar{Q}_i$.

5 Illustrative example

We will now apply the results from last Section to the example from Section 2. The input dynamics is neglected and it is possible to use normalized values for all process gains. The oxygen dynamics is modelled by a first order system:

$$\dot{x} = -x + f(v) + w$$

where f is defined by

$$f(v) = \min(v, v_{crit}) \quad \text{with } v_{crit} = 1$$

In [1], tuning rules for the probing controller are given. The pulse duration and the pulse height are chosen such that the pulse response can be clearly seen in the output signal. We choose $T_p = 1$ and $u_p^0 = 1$ to get suitable variations in the dissolved oxygen signal. The desired pulse response y_r is taken to be $y_r = 0.1$. Between two pulses, the output x is controlled by means of the agitation speed w. The length T_c of the control phase depends on how fast x can be regulated by w. Using a PI controller with $T_i = 1.5$ and $K = 3$, we take $T_c \approx 3T_p = 3$. We choose a nominal gain $K = 1$ for the probing controller.

The closed-loop system state is composed of the dissolved oxygen concentration x, the internal state x_c from the agitation speed controller and the probing controller state u:

$$X = \begin{bmatrix} x \\ x_c \\ u \end{bmatrix}$$

The functions $f(\cdot)$ and $f(\cdot + u_p^0)$ induce a partition of the state space into 3 regions:

$$\mathbf{X}_1 = \{X \in R^3, u < v_{crit} - u_p^0\} = \{X \in R^3, u < 0\}$$
$$\mathbf{X}_2 = \{X \in R^3, v_{crit} - u_p^0 < u < v_{crit}\}$$
$$= \{X \in R^3, 0 < u < 1\}$$
$$\mathbf{X}_3 = \{X \in R^3, u > v_{crit}\} = \{X \in R^3, u > 1\}$$

The dynamics in each region is given by

$$A_1 = \begin{bmatrix} -0.0225 & -0.0768 & 0.0384 \\ 0.0610 & 0.2082 & 0.3959 \\ 0.0131 & 0.0451 & 0.9574 \end{bmatrix} \quad a_1 = \begin{bmatrix} 0.6321 \\ 0 \\ 0.5321 \end{bmatrix}$$
$$A_2 = \begin{bmatrix} -0.0225 & -0.0768 & -0.5937 \\ 0.0610 & 0.2082 & 0.3959 \\ 0.0131 & 0.0451 & 0.3253 \end{bmatrix} \quad a_2 = \begin{bmatrix} 0.6321 \\ 0 \\ 0.5321 \end{bmatrix}$$
$$A_3 = \begin{bmatrix} -0.0225 & -0.0768 & 0 \\ 0.0610 & 0.2082 & 0 \\ 0.0131 & 0.0451 & 0.9800 \end{bmatrix} \quad a_3 = \begin{bmatrix} 0.0384 \\ 0.3959 \\ -0.1226 \end{bmatrix}$$

It can easily be shown that the system has a unique equilibrium point that is located in the middle region.

$$X_e = \begin{bmatrix} x \\ x_c \\ u \end{bmatrix}_e = \begin{bmatrix} 0.1114 \\ 0.4180 \\ 0.8188 \end{bmatrix} \in \mathbf{X}_2$$

A simulation of the closed-loop system has been carried out and the results are shown in Figure 3. The feed rate starting at -2 is gradually increased by the controller. At time $t \approx 15$, the glucose concentration reaches the critical point and the pulse response becomes smaller. As a consequence, the feed rate is increased carefully until the size of the pulse response equals the setpoint y_r. The stationary feed rate corresponds to a glucose concentration that is just below $v_{crit} = 1$.

The stability test from Section 4 consists of 33 LMIs with 44 decisoin variables. Feasibility of the LMI system, and as a consequence stability, could be established using the *LMI Control Toolbox* for *Matlab*. Convergence to the equilibrium is guaranteed for all initial states.

As it is shown in Figure 4, the choice of the probing controller gain K influences a lot the closed-loop performance. Large K values give fast convergence but may lead to instability. In our example, instability occurs for $K > 3$.

In order to help the user for the design, an estimate of the quadratic cost $J(X_0)$ may be useful. Since the main criterion is the convergence

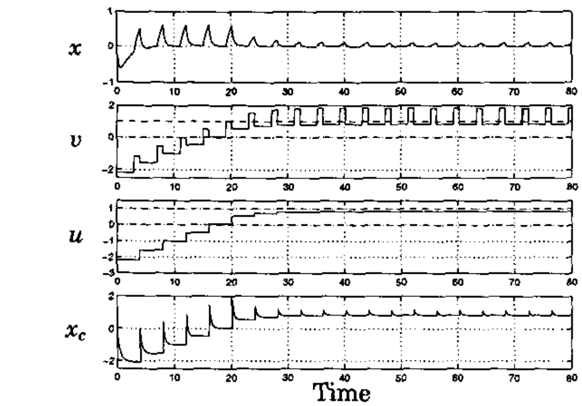

Figure 3: Simulation of the closed-loop system using the probing controller. The feed rate u is gradually increased until the response in dissolved oxygen equals the setpoint $y_r = 0.1$. At stationarity, the feed rate is just below the saturation and the dissolved oxygen signal is regulated around 0. The dashed lines represent the cell borders.

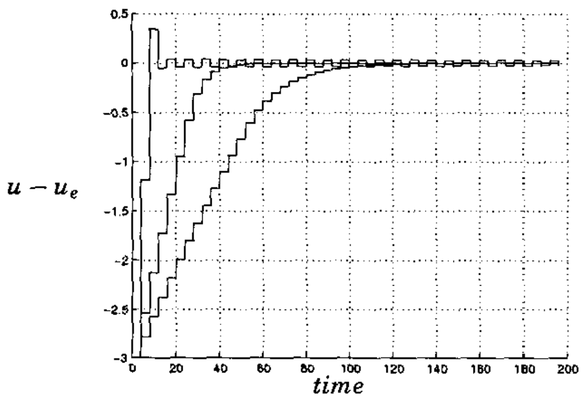

Figure 4: Shifted control signal $u - u_e$ from the probing controller for several gains: K = 0.3, 0.7, 2.97. Small gains result in a sluggish convergence while large gains may give overshoots or instability.

speed to the saturation, we choose to penalize only the third state. The matrices Q_i should also takes into consideration that the performance deteriorates much when u is above the saturation:

$$Q_1 = 2\,Q \qquad Q_2 = Q \qquad Q_3 = 4\,Q \qquad \text{with } Q = \begin{bmatrix} 0 & 0 & 0 \\ 0 & 0 & 0 \\ 0 & 0 & 1 \end{bmatrix}$$

Bounds on $J(X_0)$ have been computed for different controller gains K. The result is shown in Figure 5. The plot suggests a K value of about 2. Larger K values do not improve much the performance and may give poor robustness properties.

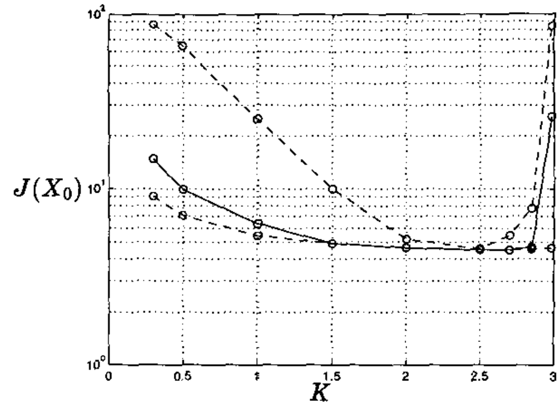

Figure 5: Transient energy $J(X_0)$ for different controller gains K. The dashed lines represent the bounds obtained by solving LMIs while the solid line was obtained from simulations. The initial state is X_0 =[0 0 -1.5]

6 Conclusion

A probing control strategy has been analysed for linear systems with an input nonlinearity that is piecewise affine. Techniques for piecewise affine systems have been used to derive stability tests of the closed-loop system. Global stability can be tested by checking the feasibility of a suitable LMI system. A method that helps the user for the design has also been presented.

Acknowledgments

This work was financially supported by the Nonlinear and Adaptive Control (NACO2) network.

A Appendix

From equation (4), we get

$$\begin{bmatrix} \dot{x} \\ \dot{x}_c \end{bmatrix} = A_{c1} \begin{bmatrix} x \\ x_c \end{bmatrix} + B_{c1} f(u_k)$$

where A_{c1} and B_{c1} are given by

$$A_{c1} = \begin{bmatrix} A + B_2 D_c C & B_2 C_c \\ B_c C & A_c \end{bmatrix} \quad B_{c1} = \begin{bmatrix} B_1 \\ 0 \end{bmatrix}$$

The matrices A_{d1} and B_{d1} are then

$$A_{d1} = e^{A_{c1} T_c} \qquad B_{d1} = \int_0^{T_c} e^{A_{c1}(T_c - \sigma)} d\sigma B_{c1}$$

One can compute A_{d2} and B_{d2} similarly and get

$$A_{d2} = e^{A_{c2}T_p} + \int_0^{T_p} e^{A_{c2}(T_p-\sigma)} d\sigma \begin{bmatrix} B_2 \begin{bmatrix} D_c C & C_c \end{bmatrix} \\ 0 \end{bmatrix}$$

$$B_{d2} = \int_0^{T_p} e^{A_{c2}(T_p-\sigma)} d\sigma B_{c2}$$

where A_{c2} and B_{c2} are

$$A_{c1} = \begin{bmatrix} A & 0 \\ 0 & 0 \end{bmatrix} \quad B_{c1} = \begin{bmatrix} B_1 \\ 0 \end{bmatrix}$$

References

[1] Mats Åkesson. *Probing Control of Glucose Feeding in Escherichia coli Cultivations*. PhD thesis, Department of Automatic Control, Lund Institute of Technology, Sweden, December 1999.

[2] Mats Åkesson and Per Hagander. A simplified probing controller for glucose feeding in *Escherichia coli* cultivations. In *The 39th IEEE Conference on Decision and Control*, volume 1, pages 4520–4525, December 2000.

[3] G. Ferrari-Trecate, F. A. Cuzzola, D. Mignone, and M. Morari. Analysis and control with performance of piecewise affine and hybrid systems. In *Proceedings of the American Control Conference*, volume 1, pages 200–205, 2001.

[4] G. Ferrari-Trecate, F. A. Cuzzola, D. Mignone, and M. Morari. Analysis of discrete-time piecewise affine and hybrid systems. *Automatica*, 38(12):2139–2146, 2002.

[5] Mikael Johansson. *Piecewise Linear Control Systems*. PhD thesis, Department of Automatic Control, Lund Institute of Technology, Sweden, March 1999.

[6] Mikael Johansson and Anders Rantzer. Computation of piecewise quadratic lyapunov functions for hybrid systems. *IEEE Transactions on Automatic Control*, 43(4):555 –559, April 1998.

[7] M. Krstic. Performance improvement and limitations in extremum seeking control. *Systems & Control Letters*, 39:313–326, 2000.

[8] M. Krstic and H-H. Wang. Design and stability analysis of extremum seeking feedback for general nonlinear systems. In *Proceedings of the Conference on Decision & Control*, volume 36, 1997.

[9] V. A. Yakubovich. S-procedure in nonlinear control theory. *Vestnik Leningrad Univ. Math.*, 4:73–93, 1977.